MARS CRUSTAL MAGNETISM

J.E.P. CONNERNEY[1], M.H. ACUÑA[1], N.F. NESS[2], T. SPOHN[3] and G. SCHUBERT[4]
[1]*NASA Goddard Space Flight Center, Greenbelt, MD, U.S.A.*
[2]*University of Delaware, Wilmington, DE, U.S.A.*
[3]*Westfalische Wilhelms-Universitat, Munster, Germany*
[4]*University of California, Los Angeles, CA, U.S.A.*

Accepted in final form 26 July 2003

Abstract. Mars lacks a detectable magnetic field of global scale, but boasts a rich spectrum of magnetic fields at smaller spatial scales attributed to the spatial variation of remanent magnetism in the crust. On average the Mars crust is 10 times more intensely magnetized than that of the Earth. It appears likely that the Mars crust acquired its remanence in the first few hundred million years of evolution when an active dynamo sustained an intense global field. An early dynamo era, ending in the Noachian, or earliest period of Mars chronology, would likely be driven by thermal convection in an early, hot, fluid core. If crustal remanence was acquired later in Mars history, a dynamo driven by chemical convection associated with the solidification of an inner core is likely. Thermal evolution models cannot yet distinguish between these two possibilities. The magnetic record contains a wealth of information on the thermal evolution of Mars and the Mars dynamo, but we have just begun to decipher its message.

1. Introduction

The Mars Global Surveyor magnetic field investigation provided the first unambiguous detection of the magnetic field associated with Mars (Acuña *et al.*, 1998). Mars presently has no significant global-scale magnetic field of internal origin, as would be expected of a source in the deep interior, e.g., an active dynamo. Remarkably, the magnetic field of Mars is crustal in origin, resulting from the variation in remanent magnetization of the crust. The most intense magnetic fields appear in association with the heavily-cratered southern highlands (Acuña *et al.*, 1999), although extended regions surrounding the giant impact basins Argyre and Hellas appear weakly magnetized or non-magnetic. Likewise, the magnetic field of crustal origin over much of the northern lowlands is relatively weak, but significant sources have been mapped at high northern latitudes (Acuña *et al.*, 1999) along the 330 deg West longitude meridian.

A similar hemispheric dichotomy is reflected in Mars geology. Terrain north of the dichotomy boundary is apparently lightly cratered and presumably younger, topographically smooth and flat, and low in elevation (Smith *et al.*, 1999). Terrain south of the boundary is heavily cratered and presumably older, more rough at all spatial scales and at high elevation. Relative ages across the dichotomy boundary have become less certain with the discovery of faint topographical features called

Space Science Reviews **0:** 1–33, 2004.

'quasi-circular depressions' in both hemispheres (Frey *et al.*, 1999). If these are counted as vestigial remains of ancient craters, the underlying crust in the northern lowlands might be a great deal older than suggested by surface appearance. The northern lowlands are thought to have experienced sedimentary or volcanic resurfacing in the Late Hesperian and Amazonian ages. The origin of the crustal dichotomy remains a mystery, one that is fundamental to Mars evolution. It has been attributed to a large impact (Wilhelms and Squyres, 1984) or impacts (Frey and Schultz, 1988) and alternatively to tectonic processes (Wise *et al.*, 1979; Sleep, 1994). The similar apparent dichotomy in crustal magnetization gives some hope that the magnetic record, correctly deciphered, can help solve one of the most important outstanding questions of Mars evolution. How did the crust form?

1.1. PRIOR OBSERVATIONS

There have been in excess of 30 attempted missions to planet Mars, beginning with an unnamed Soviet probe launched in 1960 (Table I). Only 1 in 4 achieved any measure of success, a grim reminder of the difficulty of planetary exploration, particularly in the early days of space exploration. In the last decade, the demonstrated rate of success has improved to about 50%.

The first successful mission to Mars was that of the USA spacecraft Mariner 4, which passed within 4 Mars radii on July 15, 1965. The magnetic field was indistinguishable from that of the undisturbed interplanetary environment, with no indication of a Mars magnetosphere, magnetopause or bow shock (Smith *et al.*, 1965). Thus Smith *et al.* set an upper limit on a present-day magnetic dipole moment of 3×10^{-4} Me (Me is the Earth's dipole moment, 8×10^{25} G cm^3), equivalent to an equatorial field of less than 100 nT.

For the next 32 years, despite numerous opportunities, no space probe instrumented to measure magnetic fields would pass close enough to the planet's surface to establish the presence of an intrinsic magnetic field. Soviet spacecraft were all instrumented to measure magnetic fields, and while Mars 2, 3 and 5, and Phobos 2 returned useful magnetic field data, they did not pass close enough to unambiguously detect an intrinsic field. The first US Mars missions were instrumented with magnetic sensors, but like the early Soviet missions, they either failed or remained too distant. Beginning with the launch of Mariner 6 in 1969, and excepting Mars Observer (MO) and its replacement, Mars Global Surveyor (MGS), spacecraft and landers sent by the USA to Mars did not carry magnetometers. The very successful Viking orbiters, with periapses at an altitude of 300 km, would surely have detected the crustal magnetic field in 1976 had they carried magnetometers.

The lack of a definitive measurement in the thirty years leading up to MGS, and the great interest in the question of Mars magnetism, spawned an enormous body of literature and much debate on the subject. By all accounts, the intrinsic magnetic field of Mars had to be quite small, so as to not produce a well developed and easily identified magnetosphere like that of Earth. But was a modest intrinsic

TABLE I

Chronology of Mars mission attempts[a]

Attempt	Launch date	Name	Country	Magnetic field investigation?	Mission outcome
1	October 14 1960	None	USSR	Y	Failed to reach Earth orbit
2	October 24 1962	None	USSR	Y	Failed to leave Earth Orbit
3	November 1 1962	Mars 1	USSR	Y	Flyby June 19, 1963; telemetry failed
4	November 4 1962	None	USSR	Y	Failed to leave Earth Orbit
5	November 5 1964	Mariner 3	USA	Y	Shroud separation failure
6	November 28 1964	Mariner 4	USA	Y	Successful flyby; imagery and magnetic measurements (distant)
7	November 30 1964	Zond 2	USSR	Y	Contact lost before Mars encounter
8	July 18 1965	Zond 3	USSR	Y	No Mars encounter
9	February 24 1969	Mariner 6	USA		Successful flyby July 31
10	March 27 1969	Mariner 7	USA		Successful flyby August 5
11	March 27 1969	None	USSR	Y	Launch Failure
12	April 14 1969	None	USSR	Y	Launch failure
13	May 8 1971	Mariner 8	USA		Launch failure
14	May 10 1971	Kosmos 419	USSR	?	Failed to leave Earth orbit
15	May 19 1971	Mars 2	USSR	Y	Orbited Mars; descent module crashed
16	May 28 1971	Mars 3	USSR	Y	Orbited Mars; descent module landed, telemetry failure
17	May 30 1971	Mariner 9	USA		MOI November 13; successful mission
18	July 21 1973	Mars 4	USSR	Y	Failed to orbit Mars
19	July 25 1973	Mars 5	USSR	Y	Orbited Mars; partially successful mission
20	August 5 1973	Mars 6	USSR	Y	Flyby; descent module landed, little data
21	August 9 1973	Mars 7	USSR	Y	Flyby; descent module missed Mars

TABLE 1
Continued.

Attempt	Launch date	Name	Country	Magnetic field investigation?	Mission outcome
22	August 20 1975	Viking 1	USA		MOI June 19, 1976; landed July 20
23	September 5 1975	Viking 2	USA		MOI August 7 1976; landed September 3
24	July 7 1988	Phobos 1	USSR	Y	Contact lost before Mars encounter
25	July 12 1988	Phobos 2	USSR	Y	MOI January 29, 1989; lost telemetry March 27
26	September 25 1992	Mars Observer	USA	Y	Failed to achieve Mars orbit
27	November 7 1996	Mars Global Surveyor	USA	Y	MOI September 12, 1997; successful mission (currently in extended mission)
28	December 4 1996	Mars Pathfinder	USA		Landed July 4, 1997; successful mission
29	July 4 1998	NOZOMI	JAPAN	Y	Mission replan for 2004 arrival at Mars
30	December 11 1998	Mars Climate Orbiter	USA		Failed to achieve Mars orbit
31	January 3 1999	Mars Polar Lander	USA		No contact subsequent to landing attempt; No contact with 2 microprobes deployed
32	April 7 2001	Mars Odyssey	USA		MOI October 24, 2001; successful mission

[a]Entries through 1988 from Snyder and Moroz (1992).

field – almost exclusively assumed to be a planetary dipole – necessary to explain observations at Mars? The observations considered were largely those from the Soviet Mars 2, 3, and 5 probes, reviewed by Russell (1979) and Ness (1979), but also included ionospheric electron density profiles from numerous radio occultations and the Viking landers (reviewed by Slavin and Holzer, 1982). Estimates of a putative Mars dipole ranged from 0.8 to 2.55 $\times$ 10^{22} G-cm^3 (equivalent equatorial surface field of 20 to 65 nT), but the evidence was weak at best and widely criticized (e.g., Russell, 1978a, b; Ness, 1979).

The more recent Phobos 2 mission provided the closest observations (to 800 km altitude) and numerous more distant tail passages but provided 'no conclusive evidence for a magnetic field of internal origin' according to Riedler *et al.* (1989). However, others saw evidence of a planetary field in the same data (Dolginov and Zhuzgov, 1991; Slavin *et al.*, 1991; Verigin *et al.*, 1991; Mohlmann *et al.*, 1991) and the controversy did not end (e.g., Russell *et al.*, 1995; Gringauz *et al.*, 1993) until MGS entered Mars orbit in September 1997.

1.2. MARS GLOBAL SURVEYOR OBSERVATIONS

The Mars Global Surveyor spacecraft and Mission Plan were designed to recover a subset of the science objectives of the Mars Observer Mission, which ended with Mars Observer's unsuccessful orbit insertion maneuver. The Mars Observer Mission was designed to provide a direct entry into a high inclination mapping orbit at 400 km altitude. Mars Global Surveyor, in contrast, was designed to enter into a highly elliptical initial orbit, and achieve a circular (polar) mapping orbit at 400 km altitude by aerobraking in the Mars atmosphere (Albee *et al.*, 1998). This approach uses less propellant and makes more efficient use of launch mass.

Aerobraking works by using the planet's atmosphere to slow the spacecraft, reducing apoapsis by repeated passages through the atmosphere. The desired drag is obtained by adjusting the spacecraft periapsis with trim maneuvers to raise or lower the altitude of the spacecraft at closest approach, targeting the appropriate atmospheric density. As a result of a spacecraft anomaly experienced early in the mission, MGS used many more drag passes (891 in all) than was originally intended to slow the spacecraft. The magnetometer investigation was an unintended beneficiary of the revised MGS mission plan, which allowed a far greater sampling of the magnetic field well below the nominal 400 km mapping phase altitude.

This rather unique set of circumstances resulted in a mission that can best be described in three distinct mission modes, separated by orbital characteristics (Table II). The aerobraking phases (AB1 and AB2) occurred with the spacecraft in elliptical orbit about Mars and these mission phases provided in-situ observations along most of the orbit, extending down to altitudes of as little as 100 km. During each aerobraking pass MGS acquired measurements of the vector magnetic field along the orbit track at varying altitude above the surface. These passes are distrib-

Table II.
Mars global surveyor mission phases

Phase	Begin date Year mm day (DOY)	End date Year mm day (DOY)	Mapping cycles
	Pre-mapping		
ab1	1997 09 13 (256)	1998 03 25 (084)	
spo1	1998 03 26 (085)	1998 05 27 (147)	
spo2	1998 05 28 (148)	1998 09 22 (265)	
ab2	1998 09 23 (266)	1998 03 08 (067)	
	Mapping		
map1	1999 03 09 (068)	1999 06 01 (152)	1–3
map2	1999 06 02 (153)	1999 08 24 (236)	4–6
map3	1999 08 25 (237)	1999 11 16 (320)	7–9
map4	1999 11 17 (321)	2000 02 08 (039)	10–12
map5	2000 02 09 (040)	2000 05 02 (123)	13–15
map6	2000 05 03 (124)	2000 07 25 (207)	16–18
map7	2000 07 26 (208)	2000 10 17 (291)	19–21
map8	2000 10 18 (292)	2001 01 31 (031)	22–24 (25)[a]
	Extended Mapping		
ext1	2001 02 01 (032)	2001 04 03 (093)	(25)[a] 26–27
ext2	2002 04 04 (094)	2001 06 26 (177)	28–30
ext3	2001 06 27 (178)	2001 09 18 (261)	31–33
ext4	2001 09 19 (262)	2001 12 11 (345)	34–36
ext5	2001 12 12 (346)	2002 03 05 (064)	37–39
ext6	2002 03 06 (065)	2002 05 28 (148)	40–42
ext7	2002 05 29 (149)	2002 08 20 (232)	43–45
ext8	2002 08 21 (233)	2002 11 12 (316)	46–48
ext9	2002 11 13 (317)	2003 02 04 (035)	49–51
ext10	2003 02 05 (036)	2003 04 29 (119)	52–54
ext11	2003 04 30 (120)	2003 07 22 (203)	55–57

[a]map8 was extended through the end of primary mission to include part (3/4) of the next mapping cycle (25)

uted more or less randomly over the surface of Mars and provide a sparse sampling of the field nearest the surface.

The pre-mapping mission phase included 'Science Phasing Orbits' (SPO1 and SPO2), during aerobraking operations, in which the spacecraft was 'parked' at a fixed periapsis awaiting the next mission phase. The SPO orbits provided relatively dense sampling of the vector field above the north pole of Mars at altitudes between 170 and 200 km. Mapping phase observations began in March, 1999 and continued for a full Mars year (687 days), through the end of January 2001, the end of

the MGS Primary Mission. Since then the mission has operated, and continues to operate, in extended mission, nearing the end of the second Mars year in mapping operations. The mapping phases provided abundantly oversampled coverage of the magnetic field at a nominal altitude of 400 km (370 km–438 km) and fixed (2 am –2 pm) local time.

The mapping phases, and extended mapping phases, listed in Table II nominally consist of 3 mapping cycles each (with the exception of map8 and ext1). A mapping cycle is 28 days long and provides coverage of the entire planet by repeated application of a 7 day near-repeat cycle (Albee *et al.*, 2001). The 7 day cycle consists of 88 orbits, each crossing the equator 28.6 deg westward of the previous orbit. At the end of a 7 day repeat cycle, the spacecraft ground track is displaced eastward by a nominal 242 km from the initial ground track. Subsequent cycles 'fill in the gaps', providing under ideal conditions ground tracks crossing the equator every 3 km (1 deg longitude = 59.2 km) at the end of 1 Mars year.

From the perspective of mapping a potential field, this is a particularly generous spatial coverage and a very desirable pattern of mapping. The density of sampling greatly exceeds that necessary to follow variations in the magnetic field of crustal origin with position (at orbit altitude). The spatial resolution needed to map a potential field scales with the altitude of observation; for example, a survey at 400 km altitude measures variations of comparable scale (e.g., Blakely, 1995) and need not be mapped at 3 km resolution. Just how densely the field needs to be sampled depends also on the quality or signal-to-noise (S/N) of the measurement, higher quality measurements allowing for increased spatial resolution. So there is ample opportunity to average the field over many nearby samples to achieve improved signal fidelity, reducing 'noise' from external sources. The mapping scheme is well suited for this, providing widely separated orbit tracks and a relatively long interval of time between nearby samples. For example, it takes 7 days to return to within 242 km of a particular location on the equator. This greatly exceeds the correlation length of variations ('noise') due to external sources, so to a first approximation physically adjacent (in longitude) samples may be treated as if they are statistically independent.

1.2.1. *MGS Aerobraking Observations*

An early MGS aerobraking pass is shown in Figure 1, where the spacecraft trajectory and the vector magnetic field both appear in projection on the sky as viewed from the Sun. The magnetic field is illustrated by a vector originating at the spacecraft position at 3-s intervals along the trajectory. This example, from the 6th orbit of MGS on day 264 of 1997, was the first pass over the crust of Mars to unambiguously establish the nature of the magnetic field of Mars. From this image one can see that the magnetic field of Mars is not global in scale, as it would necessarily be if it were generated in the deep interior, for example by a dynamo. Instead, for this and many other examples one finds that the spatial scale of the observed field is comparable to the altitude of observation. This is what one expects of mag-

AUTHOR!
Please notice that this figure
will be printed in colour!

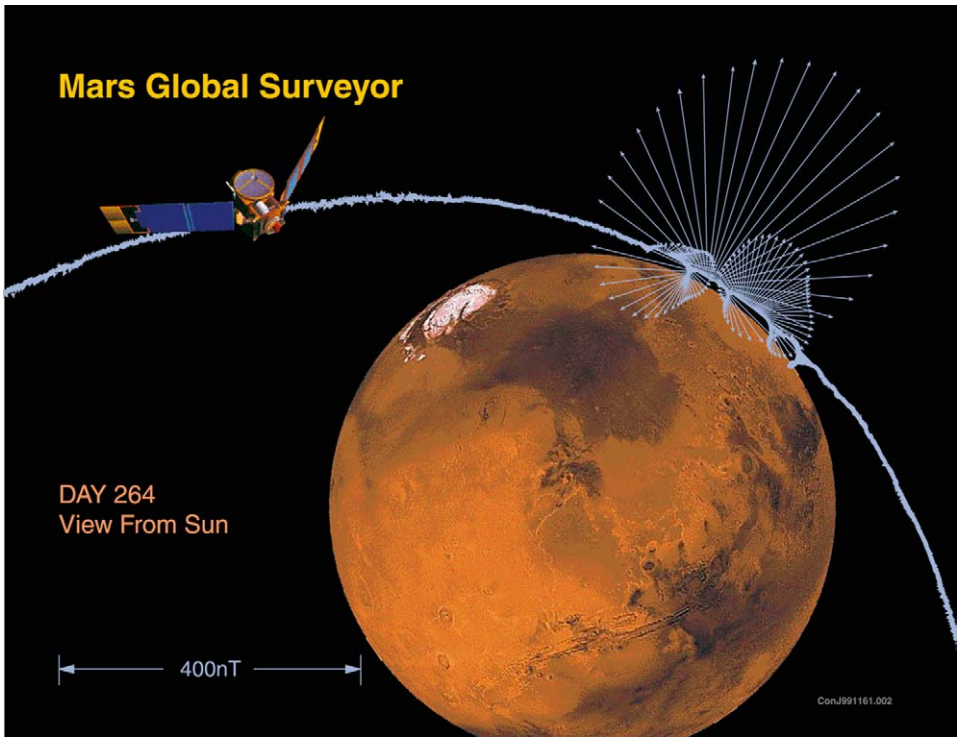

Figure 1. Projection of the MGS spacecraft trajectory and observed magnetic field onto a plane perpendicular to the Mars–Sun line and the Mars orbit plane for periapsis pass 6, 1997 day 264. The magnetic field is illustrated at 3 s intervals by a scaled vector projection of **B** originating from the spacecraft position at such times.

netic sources located near the surface of the planet, i.e., in the crust of Mars. The magnetic field of Mars is dominated by intensely magnetized sources distributed, non-randomly, in the Mars crust (Acuña *et al.*, 1998, 1999).

The MGS MAG-ER investigation obtained nearly continuous data coverage throughout most of the pre-mapping phase of the mission, with particular emphasis on acquisition of data near periapsis, as this presented a unique opportunity to sample the field at low altitudes (Albee *et al.*, 2001). Magnetometer data were acquired during 127 of 197 periapsis passes occurring in ab1; 60 of 130 passes in spo1; 211 of 244 passes in spo2; and 896 of 1111 passes in ab2. During each pass the field was sampled at low altitudes along a limited ground track centered on the latitude and longitude of periapsis and extending approximately ± 25 deg north and south of closest approach. The latitude of periapsis, about 30 deg N at the beginning of ab1, progressed slowly northward toward and over the pole through spo2. During ab2, the latitude of periapsis progressed southward, reaching a maximum of 87 deg S by the end of aerobraking. These occurred more or less randomly in longitude, so by the end of pre-mapping almost the entire surface

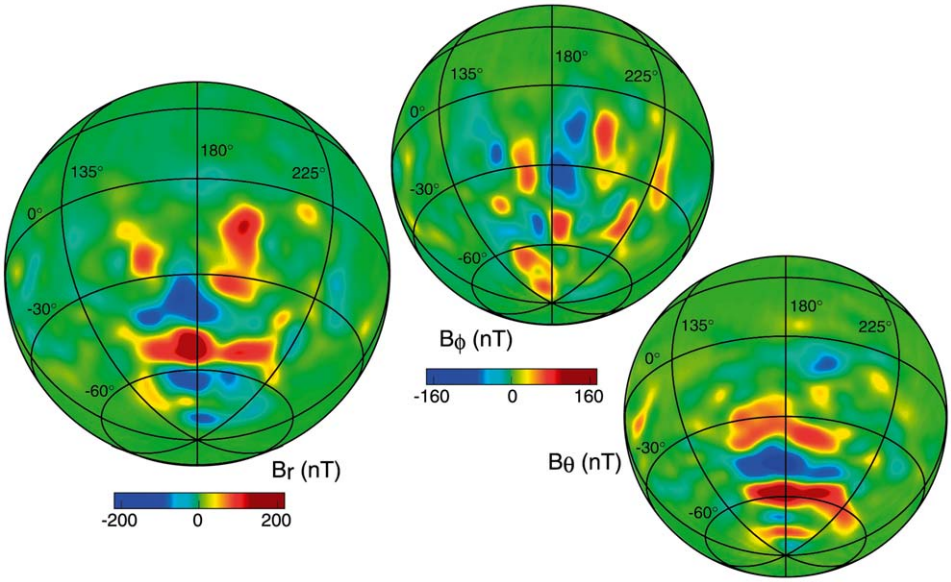

Figure 2. Orthographic projections of the three components of the magnetic field (B_r, B_θ, B_ϕ) at a nominal 400 km mapping orbit altitude, viewed from 30 deg S and 180 deg East longitude (after Connerney *et al.*, 2001).

of Mars had been sampled, albeit sparsely, at low altitude. Thus it was possible for Acuña *et al.* (1999) to map the global distribution of magnetic sources in the crust of Mars, revealing a remarkable association with the dichotomy boundary and southern highlands (see Figure 2 of Acuña *et al.*, 1999).

1.2.2. *MGS Mapping Observations*

The Mars Global Surveyor mapping phase, beginning in March of 1999, provided measurements of the vector magnetic field at nearly constant altitude (370–438 km) and fixed (2 am–2 pm) local time. These observations approximate the ideal in mapping a potential field, in that they offer a measure of the field on a closed surface about the source. A 'mapping cycle' of 28 days duration in orbit provides nearly uniform coverage of the planet with track-to-track separation of about 1 deg (59 km separation) at the equator.

At the 400 km nominal mapping altitude, magnetic fields generated by the interaction of Mars' atmosphere with the solar wind can at times be appreciable. The remainder of this volume is devoted to the study of this interaction. However, our focus in this chapter concerns the mapping of the crustal field itself and minimizing the influence of external sources on the results. To a very good first approximation, external fields draped over a conducting obstacle will align with the conducting surface, appearing largely in the horizontal component of the field. Magnetic fields generated by the solar wind interaction are time variable, reflecting variations in the solar wind, and greater in magnitude near the sub-solar point. With data from

many mapping cycles, allowing measurement redundancy and statistical reduction of external noise, the crustal magnetic field has been mapped with extraordinary signal fidelity (Acuña *et al.*, 1999, 2001; Connerney *et al.*, 2001).

Figure 2 shows a series of orthographic projections of the three components of the vector field observed in mapping orbit (Connerney *et al.*, 2001) from a vantage point located at 30 S and 180 E, above the intensely magnetized southern highlands. The map was constructed by collecting night-time observations in 1 by 1 deg lat/lon bins (59 km at the equator) and using a median value for each component as an approximation to the vector crustal field. The field due to the solar wind interaction is both quieter and weaker in magnitude over the darkened hemisphere, so elimination of dayside observations helps reduce the effects of external fields. Use of the median value for an estimate of the crustal field further reduces the effects of a time-variable external field, but it is important to note that a residual bias of a few nT remains. This residual contains some part of the global scale response of Mars' atmosphere to the solar wind (Crider *et al.*, this volume) and can also be identified in the low degree and order terms of a spherical harmonic expansion (Arkani-Hamed, 2002a). It is also important to recognize that these maps are essentially images of the observations, as opposed to images obtained from a model fit to observations, and that estimates in adjacent longitude bins are largely statistically independent. The high signal fidelity (of order 100) evident in the images is truly representative of the data.

It is interesting to compare the global maps of the crustal magnetic field of Mars (Connerney *et al.*, 2001) with those of the Earth derived from MAGSAT observations at comparable altitude (Langel *et al.*, 1982), and the more recent maps derived from Orsted (Olsen, 2002) and Champ (Maus *et al.*, 2002) at somewhat greater altitude. In the case of the Earth, the much larger internal field must first be removed, with some uncertainty, and observations need be detrended or otherwise filtered along track to remove residual internal fields as well as external fields. What remains is a crustal field at least an order of magnitude weaker than that of Mars. The Earth's magnetic anomalies must be estimated in the presence of a large inducing field, so it is not possible to distinguish between induced and remanent magnetism, except, perhaps in a statistical sense (Maus and Haak, in press). Free of such ambiguities, Mars is an ideal laboratory for the study of crustal magnetic fields and their origin.

2. Interpretation of the Magnetic Field

Before we turn to a more detailed discussion of how to interpret the crustal magnetic field of Mars, it is useful to summarize what can reasonably be inferred from the observations themselves. The lack of a present-day global field means that Mars does not now have an active dynamo in its deep interior. Since parts of the crust are intensely magnetized, it is hard to escape the conclusion that Mars once had

an active dynamo (Acuña *et al.*, 1999), whether or not remanence was acquired by thermoremanent magnetization (TRM), as seems likely, or some other process (e.g., chemical remanent magnetization, or CRM). This observation requires that Mars had a convecting, electrically-conducting core within which a dynamo operated for a geologically significant interval of time. Most models of Mars evolution would have a molten iron core forming early, after or during hot accretion some 4.5–4.6 billion years (Gyr) before the present (Schubert *et al.*, 1992; Stevenson, 2001; Spohn *et al.*, 2001; see, however, Senshu *et al.*, 2002).

It also appears likely that Mars' dynamo ceased operation relatively early in the planets evolutionary history, as suggested by Acuña *et al.* (1999), although this inference is not indisputable. Acuña *et al.* noted that expansive regions above the large impact basins (Hellas, Argyre, Isidis) lacked measurable crustal fields, as did much of the northern lowlands. For the moment let us accept the notion that this observation implies that the associated crust is not magnetized. Had these structures formed in the presence of a large ambient field, they would likely have acquired intense remanent magnetization as the rock cooled below the Curie temperature. This process would leave identifiable magnetic signatures above these features, where none is observed. Either they formed after cessation of the dynamo, or the magnetic imprint originally acquired was subsequently erased. This would require reworking the entire crust in the vicinity of these basins (e.g., reheating above the Curie temperature or demagnetization by shock) without leaving a visible trace. The formation of these large impact basins is believed to have occurred about 4 Gyr ago, leading to the conclusion that the dynamo had ceased operation after just a few hundred million years.

An alternative proposal by Schubert and colleagues (Schubert *et al.*, 2000) would have the large impact basins form prior to the onset of the dynamo (see also Stevenson, 2001), reversing the chronology proposed by Acuña *et al.* (1999). This proposal was motivated, in part, by the lack of detection of a distinct magnetic signature, or 'fringing field', associated with the large impact basins (which depends on the scale length of crustal magnetization, discussed in detail in Section 2.3). Schubert *et al.* propose that the magnetization of the southern highlands arose mainly from localized heating and cooling events that post-date the era of large impacts and basin formation. They observe that early onset and cessation of the dynamo is difficult to reconcile with the notion of a dynamo driven by solidification of an inner core (as is thought to be the case for Earth). There is as yet no unambiguous observational constraint on the timing of the dynamo, but for the fact that it has existed in the past and has ceased to operate since. Whatever the cause, the dichotomy in magnetization of the Mars crust is perhaps the most significant clue in its evolution.

It is also difficult to escape the conclusion that the crust of Mars is intensely magnetized, and that the magnetization displays a coherence over hundreds of km, persisting for billions of years. This requires an iron rich crust with a magnetic mineralogy that can acquire and preserve, over aeons, a large remanent field. To-

gether with inferences on the composition of the Mars mantle from studies of the SNC meteorites (Wadhwa, 2000; McSween *et al.*, 2001), this implies an increased oxidation state relative to mantle-derived rock, consistent with assimilation of an aqueous component at crustal depths (Connerney *et al.*, 2001).

These observations provide very important constraints for Mars evolution, but it is clear that there is much more to be learned if the magnetic record in the Martian crust can be deciphered. In the following sections we consider models of the magnetic field, both global and regional, and what might be learned from them.

2.1. BASIC CONCEPTS

Interpretation of the magnetic field is an exercise in the field of potential theory, the study of harmonic functions that are solutions of Laplace's equation. They often arise in studies of gravity, magnetic and electric fields, and problems of heat and fluid flow, for example (Kellogg, 1929; Blakely, 1995). The principle of superposition holds for harmonic functions, so given a distribution of sources (e.g., magnetic dipoles) one can compute the field throughout space by summing up that due to individual sources or by integration over a volume. Theorems of uniqueness on harmonic functions ensure that a potential is uniquely determined within a closed regular region by its values on the boundary of that region, or, with some restriction and to within an additive constant, by the values of its normal derivative on the boundary (e.g., Kellogg, 1929). Alternatively, if the potential and its normal derivative are known on any arbitrary surface, it is uniquely determined in the three dimensional neighborhood of any point of that surface. So, for example, the properties of such functions can be used to continue the field from one surface to another, as is often done in geophysical surveys, apart from practical concerns.

However, the distribution of sources is not determined by knowledge of the potential, however complete. A potential can be due to various source distributions. As a simple example, consider the magnetic field of a dipole at the origin and that of a uniformly magnetized sphere of radius a. Observed in a region exterior to the sphere, both source distributions produce the same (dipole) magnetic field and are therefore indistinguishable. In general, given a source some distance from the point of observation, there is always an alternate source distribution nearer the point of observation that can approximate to any desired accuracy the field of the more distant source. So, for example, when fitting an observed field with a dipole source at some depth in the crust, it is likely that the true source is both closer to the observer (not as deep in the crust) and spatially distributed.

One may also point to sources that produce no magnetic field, and by superposition show that any model is non-unique. The magnetic field external to a uniformly-magnetized infinite plate is zero (e.g., Blakely, 1995). This might be a good approximation if the observer is close to a uniformly-magnetized source, compared to its extent. Such a plate with a hole in it produces the same field

as an isolated, uniformly magnetized (in the opposite sense) disc sized to fit the hole. This works as well with a spherical cavity; a dipole field observed above the crust might equally well indicate a hole in such a plate or an isolated, uniformly magnetized sphere of the same size.

Consider a spherical shell (e.g., planetary crust) in which the intensity of magnetization is constant and the direction of magnetization is everywhere radial. Symmetry and Gauss' theorem dictate that the magnetic field produced by such a source is zero. In fact, there are infinitely many ways to magnetize a spherical shell (and therefore a solid sphere) in such a way as to produce no magnetic field exterior to the shell (Runcorn, 1975a, b). Runcorn's theorem states that if a shell of any thickness acquires a magnetization, the intensity of which is proportional and parallel to a magnetizing field of internal origin, which later disappears, its external field is zero (aside from practical concerns; see, e.g., Goldstein, 1975; Leweling and Spohn, 1997). Runcorn applied this theorem to argue in favor of a lunar magnetic field of internal origin. However, one can also posit a crust with many 'Runcorn spheres' of all sizes scattered about, undetectable by external measurements of the magnetic field.

Measurements of the vector magnetic field, exterior to a source region, cannot, therefore, uniquely determine the properties of the source. Additional information is required if we are to learn about the intensity and direction of magnetization, or the distribution of magnetization, within the source region (i.e., crust, or interior of a planet). The validity of a magnetization model and the utility of the model depend critically on the validity of the additional information, or constraints, imposed on the solution.

Spherical harmonic analysis is by far the most popular method used in the interpretation of potential fields of global scale, dating back to its introduction by Gauss in 1838. It is particularly useful to describe the field produced by a source distributed near the origin, and has been applied to the Earth's field (Langel, 1987) as well as all of the magnetized planets (Connerney, 1993). It is far less efficient when applied to a source distribution that is not compact, such as crustal magnetization. On a global scale, crustal sources have been modeled by fitting a large number of equally spaced dipoles in a shell approximating the crust (Mayhew and Galliher, 1982). They assumed that the Earth's crustal field is largely due to induction, the direction of each dipole being fixed by that of the main field. This constraint is not applicable in the case of Mars, where no global field exists today.

On a local scale, observations can be fit to any model for which the field can be calculated, beginning with simple dipoles, thin sheets, uniformly magnetized volumes, etc. In geophysical surveys, one often finds the direction of magnetization constrained, as appropriate for induced fields, in modeling the source. Constraints provided by local geology, gravity, seismic data, or borehole measurements and samples are often introduced to constrain the distribution of magnetization (e.g., Telford *et al.*, 1976) in applied geophysics.

2.2. GLOBAL MODELS

The first global scale model of the magnetic field of Mars was produced by Purucker and colleagues (Purucker *et al.*, 2000) using Mars Global Surveyor aerobraking phase observations. They used an equivalent source technique, representing the crustal field by superposition of many dipoles, approximately equally spaced (about 111 km apart), on a reference sphere of radius 3394 km ($\sim$ 1 R_m). The magnetization direction of all 11,550 dipoles was assigned (radial) as were the locations; only the magnitude of each was varied to fit the observations. The model was used to construct a nearly complete altitude-normalized map of the radial magnetic field at a reference altitude of 200 km. The model should be regarded as a tool for interpolating the field between orbit tracks in a manner that satisfies Laplace's equation (one of many). The model will approximate the field in the immediate vicinity of orbit tracks. At low altitudes, the calculated field would merely reveal the (arbitrary) locations of the many dipoles used to represent the field. Special care is needed to remove source dipoles that are not well constrained by the observations (too distant from the trajectory), and to identify individual passes with large external field variations, to avoid bias in the source dipoles fitted.

Spherical harmonic models of the field have been presented by Arkani-Hamed (2001a, 2002a), Cain *et al.* (2003), and Voorhies *et al.* (2002). Arkani-Hamed's model is an expansion to degree and order 50, most recently improved by addition of mapping orbit observations, while both Cain *et al.* (2003) and Voorhies *et al.* (2002) use expansions to degree and order 90. The higher the degree and order of the expansion, the greater the spatial resolution afforded by the model, in general, although one will find much discussion regarding the appropriate choice of $n_{\max}$ for a specific dataset. Arkani-Hamed (2002) represents the spatial resolution afforded by a 50-deg expansion as comparable to a wavelength of 420 km on the surface and argues that this is the maximum resolution afforded by the data. However, Cain *et al.* (2003) show several examples of low-altitude aerobraking data that are reasonably well fit by their 90-deg spherical harmonic model and poorly represented by an expansion limited to 50-deg.

Like the many-dipoles equivalent source models, the spherical harmonic models provide a useful tool for interpolating the field in the general vicinity of the orbit tracks along which the original data were acquired. Upward continuation of the field with a spherical harmonic expansion can be expected to work well, within a region devoid of local currents, providing that the external field is also taken into account. At the 400 km altitude of the mapping mission, MGS spends about half its time above the ionopause (Mitchell *et al.*, 2001), and local currents due to the interaction of the atmosphere and crustal field with the solar wind are already significant.

In contrast, downward continuation of a spherical harmonic model works well only for compact sources, i.e., fields due to sources deep in the interior. The (unmodeled) magnetic field associated with small spatial scale variations in crustal

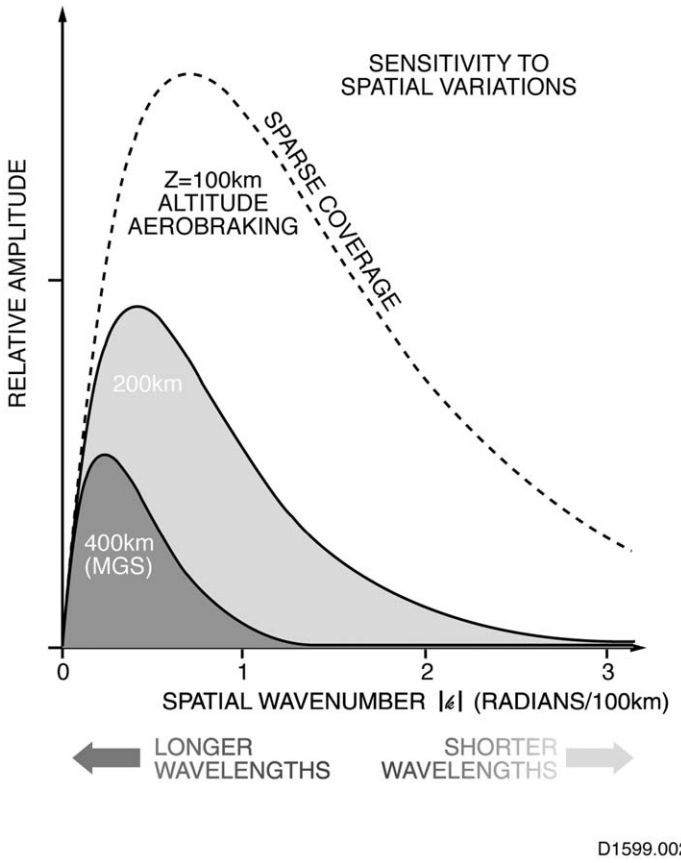

Figure 3. Sensitivity to spatial variations in magnetization depends on the altitude of observation. We compare the relative amplitude of crustal signals as a function of spatial wavenumber (wavelength) for three different mapping altitudes. Peak sensitivity shifts to shorter wavelengths as altitude decreases (after Blakely, 1995).

magnetization grows exponentially larger as one continues downward. Such fields will quickly overtake those associated with large spatial scales. Indeed, the altitude of observation essentially selects a range of observable spatial wavelengths, comparable to the survey altitude; signals associated with smaller spatial scales, *and* longer spatial scales, are greatly attenuated (Figure 3). Downward continuation of a truncated spherical harmonic will do little more than slightly alter the field as observed at altitude, providing little additional insight. Any information about small spatial scales – those that will be far more prominent near the surface – has already been removed from the data!

Figure 3 is a good illustration of the power of altitude in a geophysical survey, or in our application, the global mapping of a planet. The altitude of the mapping orbit determines the wavelength of spatial variations that the survey will be most sensitive to; lower altitudes favor higher spatial resolution. The curve correspond-

ing to 100 km altitude (reached in aerobraking) is rendered with a dashed line to distinguish it from those (at 200 km and 400 km) that correspond to practical circular orbit altitudes. The atmospheric drag at 100 km altitude on Mars is much too large for completion of a global survey at that altitude. A collection of aerobraking passes provides a wealth of information but these data cannot be continued without additional information, in contrast to high-fidelity measurements on a surface.

The spatial resolution afforded by a complete survey at a particular altitude is easily deduced from Figure 3. The commonly-held view is that the spatial resolution afforded by a survey is comparable to the survey altitude. This is about right in the case of the Earth, where fields of crustal origin must be measured, with considerable difficulty, in the presence of the much larger background field, resulting in limited signal-to-noise maps. In this case, for S/N ratios of a few, the spatial resolution obtained is comparable to that of the peak amplitude, at about 1 radian per h where h is the mapping altitude. However, if you measure the field with much higher signal-to-noise, you gain information at spatial scales above and below the peak. The highest spatial resolution afforded by the survey is obtained by following the curve in Figure 3 to the right until the amplitude is reduced by a factor comparable to the S/N of the map. For the MGS mapping of Mars at 400 km altitude (Connerney *et al.*, 2001) the vector field has been mapped with extraordinary signal fidelity (S/N $\sim$ 100), yielding information to spatial scales of about 1 radians/100 km.

The global representations will be most useful in studies of the solar wind interaction with Mars, where details of the field below mapping altitude are less important. The global representations, it should be noted, are very inefficient when applied to crustal sources, which by nature are local. The magnetization acquired and preserved in the crust is strongly dependent on the rock composition and mineralogical form of the iron, its magnetic microstructure, magnetizing field intensity, and the subsequent chemical, thermal, and mechanical history of the sample. These are largely localized phenomena with small spatial scales, compared with satellite mapping altitudes. An isolated source is more easily and accurately described by a simple dipole than with a set of orthogonal basis functions (spherical harmonics) spanning the globe. For example, a spherical harmonic expansion to $n_{\max} = 90$ requires $(n_{\max} + 1)^2 - 1 = 8280$ coefficients to fit such a source where 6 free parameters would do better.

For this reason, we prefer regional analyses and source modeling techniques, described in the next section, to address crustal magnetization. However, spherical harmonic analyses can provide a useful representation for some applications and an interesting comparison with Earth's crust. Figure 4, from Voorhies *et al.* (2002), shows a comparison of the 'magnetic spectra' of Earth and Mars, i.e., the mean-square amplitude of the field due to harmonics of degree n as a function of n. The Earth's spectrum for $n < 13$ or so is identified with the core field, produced by the dynamo below 0.55 the planet's radius. The higher degree terms are identified with crustal sources (Langel and Estes, 1982) and are reasonably well fit by a

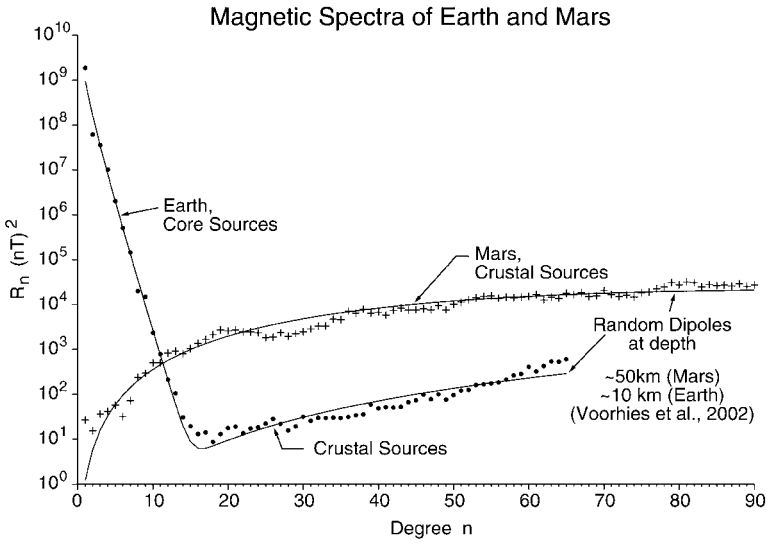

Figure 4. Mean square amplitude of the magnetic field on the surface of a sphere (radius a) from spherical harmonics of degree n for Earth ($a = 6371$ km) and Mars ($a = 3394$ km). The fitted curve for the Earth is the sum of spectra from core sources (dynamo) and that of a crustal source shell of random dipoles at shallow depth. The fitted curve for Mars is that of a source shell of random dipoles in the crust only (after Voorhies *et al.*, 2002).

distribution of random dipoles near the surface (top 18 km of crust). In contrast, the entire Mars spectrum is well described by a random distribution of dipoles at a depth of about 50 km (Voorhies *et al.*, 2002) beneath the surface. Connerney *et al.* (1999) claimed that the Mars crust was an order of magnitude more intensely magnetized than Earth's, on average. Voorhies *et al.* (2002) show more precisely that the Mars crust is a factor of 9.6 ($\pm$ 3) more intensely magnetized over all spatial scales for which a comparison is possible.

2.3. SOURCE MODELS

Perhaps the most fruitful way one might address crustal magnetization is through the use of source models, whereby the field produced by a volume of magnetized material is compared with that observed. Of course, one must be cognizant of the non-uniqueness inherent in potential field modeling, and critical of any assumptions made to constrain the range of solutions. However, source modeling allows for the introduction of additional constraints based on other knowledge, where appropriate. In general, magnetic survey data can be enhanced with knowledge of local geology, sample measurements, gravity, borehole measurements and samples, and so on. This is why *forward modeling* is so popular in geophysical surveys. It is relatively easy to incorporate such constraints into the model, e.g., constraining the volume and location of magnetized material, or the direction of magnetization (induced fields), or intensity of magnetization (if one has samples).

In the case of Mars, we currently have few if any constraints applicable on a scale appropriate to the observations. Most of the Mars data is acquired at about 400 km altitude, supplemented by aerobraking data down to about 100 km altitude. We are thus limited to spatial scales *roughly* comparable to 100 km (Figure 3) and require constraints of comparable scale. It is difficult to imagine a source of such dimensions with uniform magnetization, for example, or uniform direction of magnetization. However, one can envision the wholesale demagnetization of the crust in the vicinity of large impact craters and basins, many of which have appropriate spatial scales (e.g., Acuña *et al.*, 1999).

It may be worthwhile to digress briefly to address questions of scale in more detail. Consider the regional demagnetization of the crust in the vicinity of the major impact basins (e.g., Hellas, Argyre, Isidis), used by Acuña *et al.* (1999) to establish constraints on the history of the dynamo. They assumed that crustal remanence was erased by a thermal event or shock demagnetization, or both, associated with the large impact events. The magnetic field mapped over these regions is very weak or non-existent, compared to that in neighboring regions where variations in the field are large over a range of spatial scales appropriate to the mapping altitude. This is the expected result if the crust was characterized throughout by variations in magnetization over a broad range of spatial scales, subsequently erased in the vicinity of the large impact basins (diameter 1000–2000 km). This interpretation requires that the spatial scale of the largest basins exceed that of the spatial variations in crustal magnetization.

The opposite extreme in spatial scales would lead to a very different conclusion. Suppose that the crust were uniformly magnetized throughout, so that the spatial scale of variations in crustal magnetization greatly exceeded that of the largest impact basins. In this case, demagnetization of a circular disc associated with the impact event would produce a 'hole' in the otherwise uniformly magnetized infinite plate. Mapped at an altitude significantly less than the dimensions of the disc, the magnetic field would simply reveal the edge of the disc, tending to zero towards the center of the disc and away from the rim (Ochadlick, 1991). This kind of signature is not evident in the MGS observations (Acuña *et al.*, 1999; Arkani-Hamed, 2001a). The lack of such a signature led Schubert *et al.* (2000) to argue against the possibility of an early Mars dynamo. The disparate interpretations result directly from different assumptions regarding the relative spatial scales.

Figure 5 shows examples of uniformly magnetized sources and the fields observed along a traverse above them. The fields produced by the sphere and long cylinder at a depth d are similar, but the cylinder can be distinguished by the relative amplitudes of horizontal and vertical fields, and by the less rapid decay of the field with distance from the source. The depth of the source in both cases can be estimated from the peak-to-peak separation of the field (either component, depending on magnetization direction) in the ideal case. The thin plate example shows a traverse just above the plate (depth $\ll$ width) to illustrate the edge effect visible in passing over a uniformly magnetized source at an altitude that is much

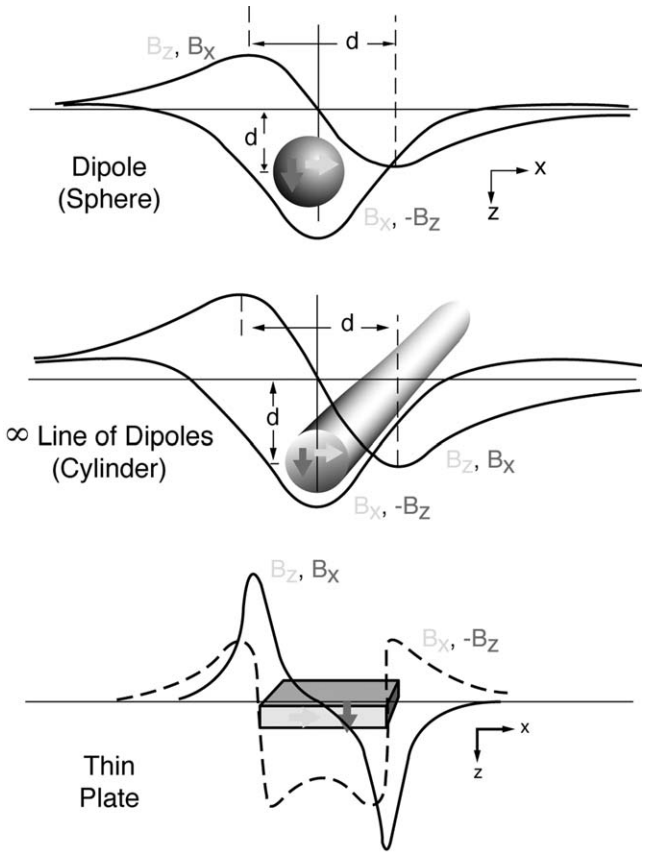

Figure 5. Magnetic field above some simple sources (red labels for $+z$ direction of magnetization, blue for $+x$) (a) dipole source, equivalent to a uniformly magnetized sphere, at depth d (b) infinite line of dipoles, or uniformly magnetized cylinder, at depth d (c) uniformly magnetized thin plate, at depth 0.1d.

less than the width of the plate. In exploration geophysics, the horizontal gradient of the field is often used to outline separate sources. A traverse above the same source at depth comparable to or greater than the width would look much like those above.

In source modeling, one attempts to learn something about the source by fitting one or more such simple sources to the observed vector field. It is very common in exploration geophysics to approximate more complex sources by summation over many uniformly magnetized thin plates. Connerney *et al.* (1999) fit a source model to the vector data acquired by MGS at low altitude (to 100 km) over the intensely magnetized southern highlands. The magnetic field observed over this region is organized in east-west-trending lineations, some extending over 2000 km in length. A remarkably good fit to the vector data acquired during several aerobraking passes over Terra Cimmeria and Terra Sirenum was obtained using a

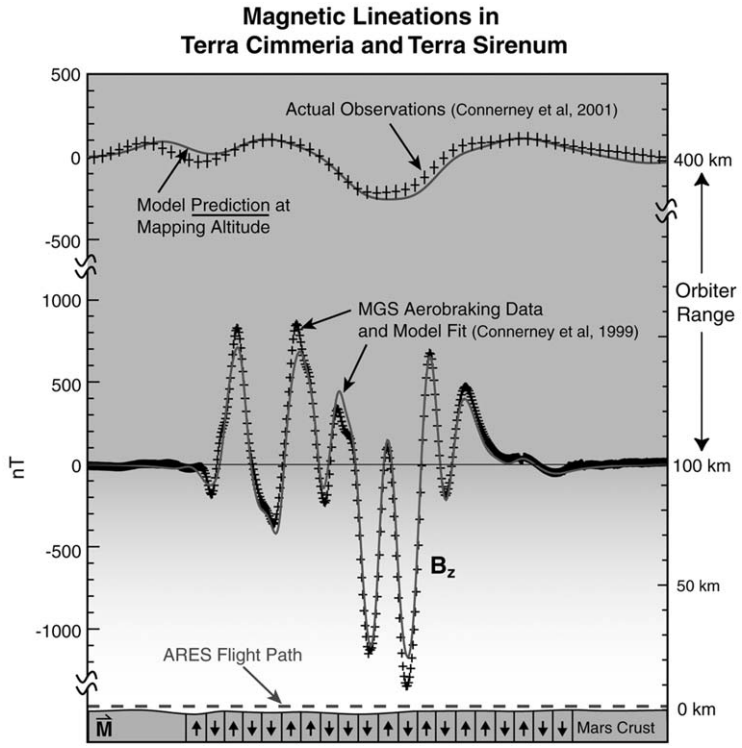

Figure 6. MGS observations (crosses) at approximately 100 km (aerobraking) and 400 km (mapping orbit) altitudes compared with that computed from the 20-plate model of Connerney *et al.* (1999). The model, fit to the aerobraking observations only, does a very good job fitting the high altitude observations obtained two years later during mapping phase. Model magnetizations indicated below are schematic only. This comparison illustrates well the rapid increase in magnitude of variations of smaller spatial scale observed at lower altitude.

multiple thin plate model. The model consisted of 20 uniformly magnetized thin (30 km) plates, 200 km in width, extending to infinity in the east-west direction (Figure 6). Plate magnetizations, obtained by least squares fitting the underparameterized linear system, varied from approximately $+20$ A m^{-1} to -20 A m^{-1}, in a pattern reminiscent of the alternating magnetic polarities observed over mid ocean ridges on Earth (Vine and Matthews, 1963).

Connerney *et al.* (1999) concluded that crustal magnetizations on Mars were at least an order of magnitude greater than those observed on Earth, and noted that the observations could be fit with a pattern of magnetization like that found on Earth in association with crustal spreading in the presence of a reversing dynamo (considered in more detail by Nimmo and Stevenson, 2000). The characteristic horizontal scale length of such features on Earth, determined by the crustal spreading rate and the characteristic time interval between dynamo reversals, is of order 10 km, a spatial scale well beyond the reach of orbiting spacecraft. Variations

of order 100 km width might result on Mars if the rate of spreading was greater and/or if dynamo reversals were less frequent, relative to Earth. Crustal spreading on Mars is expected to occur at a higher rate (Sleep, 1994), if at all, because of lower gravity (0.38 that of Earth) and slightly greater density of the mantle. Little is known of dynamo reversals, except on Earth where the time between reversals of the magnetic field has varied greatly, with a few reversals per million years being typical.

The MGS observations are sensitive to crustal magnetizations averaged over ~ 100 km scales, and it is possible that even greater magnetization contrasts, over smaller spatial scales, are responsible for the variations observed by MGS. Observations at lower altitude will be required to explore this possibility. At the other extreme, Parker (2003) developed a theory to establish the lowest possible intensity of magnetization consistent with the data modeled by Connerney *et al.*, (1999). Interpolating his results to a comparable crustal thickness, Parker finds a minimum magnetization intensity of 9 A m^{-1} is required to satisfy the MGS observations. This is an extraordinary intensity of magnetization (averaged over huge volumes of crust), compared to that found on Earth (Connerney *et al.*, 1999; Arkani-Hamed, 2001a; Kletetschka *et al.*, 2000).

Sprenke and Baker (2000) modeled the same observations under a variety of assumptions, and found that a crustal spreading model fit the observations well, particularly if a variation in magnetization intensity along the east-west direction was allowed. They too found magnetization intensities of 10s of A m^{-1}, assuming a 30 km thick crust. Their model allowed normal and reversed magnetization directions only, fixed in the direction of an assumed aerocentric dipole. They also examined models with only 1 polarity (magnetic shell concept), creating a similar field by separation of many similarly magnetized slabs. Given the insensitivity of all such models to addition or subtraction of a uniformly magnetized layer, the models differ little in practical terms; the distinction is in the mechanism of origin.

How the Mars highlands crust acquired remanence of this magnitude, and with the intriguing east-west trending (largely two dimensional) geometry, remains a mystery. Among the possibilities considered by Connerney *et al.* (1999), crustal spreading in the presence of a reversing dynamo, like sea floor spreading on Earth, is perhaps the most controversial and far reaching. This is a mechanism that is in process on Earth, and it has the potential of satisfying the need for huge volumes of intensely magnetized crust. Alternatively, the lineations may have formed as a series of volcanic or intrusive events with the appropriate geometry (Connerney *et al.*, 1999), forming giant dike swarms (Nimmo, 2000) like the fragmented dike swarms observed on Earth (Ernst *et al.*, 2001). The latter are abundant within the most ancient, Precambrian terranes on Earth, and coeval dikes can be traced from one continent to another after the continents are reconstructed by closure of the Atlantic Ocean. The formation of a series of suitable dikes on Mars is plausible (Nimmo, 2000), but even with very intense magnetization (15 A m^{-1}) they would necessarily be great in number and orders of magnitude wider than the 10 meter

width typical of terrestrial dikes (Ernst *et al.*, 2001). Relatively few large dikes have been identified on Mars, compared with Earth and Venus; those that are visible in Terra Sirenum and Terra Cimmeria are not oriented in the direction of the magnetic features.

Fairen *et al.* (2002) proposed that the magnetic lineations on Mars were formed at a convergent plate margin through collision and accretion of teranes. In their model, the strongly magnetized southern highlands are 'a jigsaw of continental and oceanic pieces' related to a past era of plate tectonics, formed by to a process of crustal convergence rather than crustal generation.

While much attention thus far has focused on the southern highlands, source models have also been developed for other regions. Hood and Zakharian (2001) have done detailed modeling of the north polar sources mapped during the SPO mission phase (Acuña *et al.*, 1998), concluding that they formed prior to the end of heavy bombardment. They also computed putative paleopoles, assuming that the sources are uniformly magnetized discs of approximately 400 km diameter. Their paleopoles lie between about 30 and 60 deg N along the 225 deg E meridian. Arkani-Hamed (2001b) isolated 10 sources, computing paleopole positions for each by fitting uniformly magnetized bodies (in the shape of an ellipsoid of revolution) of similar dimension to each. He finds a cluster of such pole positions centered on 25 deg N and 230 deg E. In contrast, Sprenke and Baker's (2000) preferred paleopole lies near the equator at the prime meridian.

All of the authors discussed above acknowledge that it is impossible to uniquely determine the direction of magnetization in the crust from the measurements available. It would seem unlikely that sources with such dimensions (~ 100 km $\times$ 30 km) are uniformly magnetized; indeed, cooling such a large body by thermal diffusion could require tens of million years. It is also likely that the actual causative bodies are non-uniformly magnetized and that they assume volumes poorly approximated by simple geometrical bodies. The intensity of magnetization, in particular, typically varies by a large factor within the same geologic formation. In general, the direction of magnetization inferred for a particular source covaries with the location, geometry, and size of the source; absent *a priori* knowledge or geophysical constraints, such determinations need be viewed with caution.

3. Implications for Mars Interior and Evolutionary History

The observation of strong remanent crustal magnetization provides useful constraints on the interior structure and evolution of Mars. It is generally accepted that terrestrial planetary magnetic fields are produced by regenerative dynamo action in a fluid iron-rich core or outer core shell. The observation of strong crustal remanence thus provides further evidence for the existence of an iron-rich core. Models of Mars' interior structure (e.g., Goettel, 1981; Sohl and Spohn, 1997) have cores with radii between 40% and 50% of the planetary radius. There is little doubt that

the core formed early (Schubert *et al.*, 1992; Stevenson, 2001; Spohn *et al.*, 2001). Pb and H/W isotope data (Chen and Wasserburg, 1986; Lee and Halliday, 1997; Kleine *et al.*, 2002) suggest that the core formed contemporaneous with accretion or within a few 10 million years thereafter.

The Earth's dynamo is thought to be driven by vigorous thermal and compositional convection associated with the freezing of the solid inner core. Numerical calculations (e.g., Glatzmeier and Roberts, 1997; Roberts and Glatzmeier, 2000) have shown that both thermal and compositional convection can drive a dynamo. Thermal convection in the liquid part of the core is driven by a sufficiently large super-adiabatic temperature gradient in the core. Because the core fluid has a comparatively low viscosity (approximately 1 Pa s), only a small super-adiabatic temperature difference across the core is required. This arises naturally when mantle convection removes heat from the core at a sufficiently large rate. This heat flow must be larger than the heat flow supplied by thermal conduction along the core adiabat. The latter therefore serves as a lower limit, below which thermally driven convection in the core is not supported. The critical value of core heat flow depends on the adiabatic temperature gradient in the core and the thermal conductivity. Nimmo and Stevenson (2000) estimate the critical heat flow for the Martian core to be between 5 and 20 mW m^{-2}.

In the present Earth, latent heat release at the inner core-outer core boundary probably keeps the core super adiabatic (Stevenson *et al.*, 1983; Buffet *et al.*, 1996). Estimates of the growth rate of the Earth's inner core suggest that the inner core is substantially younger (1–2 Gyrs of age) than the oldest magnetized continental crust rocks (> 3.5 Gyrs). If the inner core is indeed this young, then the Earth's early dynamo was driven by cooling and thermal convection alone without the latent heat and chemical buoyancy supplied by the inner core. Alternatively, the Earth's inner core could be substantially older if the core contains radiogenic heat sources. By analogy, either a purely thermally driven dynamo or a dynamo driven by latent heat release and chemical buoyancy might have operated in the Martian core.

A comparison of two thermal history models of Mars appears in Figure 7. This figure shows the heat flow from the core as a function of time calculated for two different evolutionary models of Mars (Breuer and Spohn, 2003). The first model type assumes that Mars had an early epoch of plate tectonics for about 500 Myr after accretion and core formation (see also Nimmo and Stevenson, 2000). That epoch ended with a transition to the present tectonic style, which is characterized by an immobile or stagnant lid, under which convection continues in the mantle. Heat transfer under these conditions, including strongly temperature dependent mantle viscosity, has become known as stagnant lid convection (e.g., Solomatov, 1995; Grasset and Parmentier, 1998). The second model type assumes that stagnant lid convection prevailed throughout the entire evolution of Mars. Two curves are drawn for each model type, differing in the assumed initial temperature difference between the core and the mantle evaluated at the core mantle boundary.

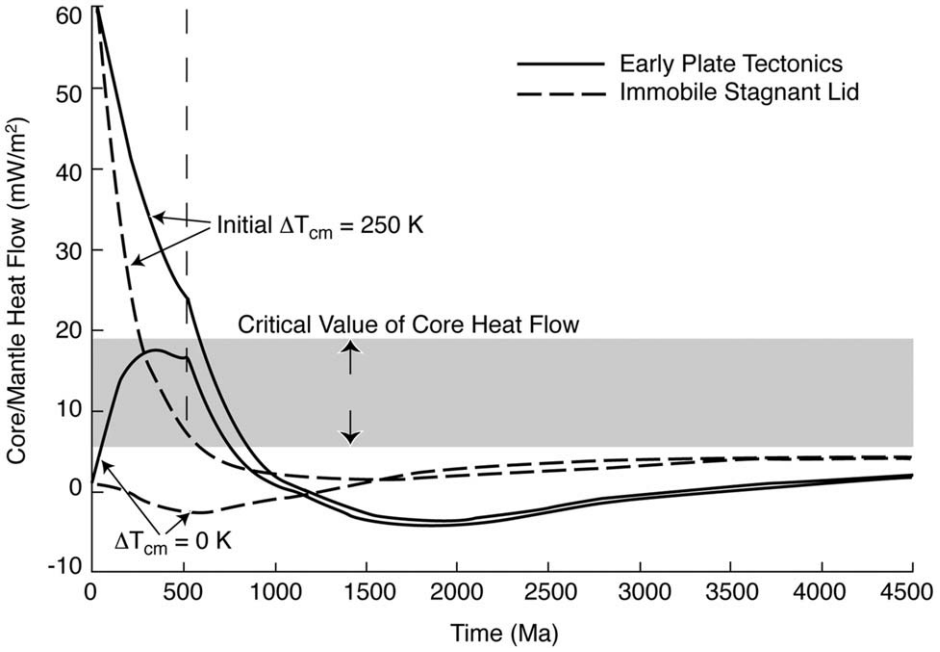

Figure 7. Core/mantle heat flow as a function of time for models of Mars evolution. Solid line: models with an early epoch of plate tectonics followed after 500 Myr by the formation of an immobile stagnant lid or lithosphere above the (convecting) mantle. Dashed line: models with an immobile stagnant lid throughout Mars history. Two curves are drawn for each model, differing in the assumed initial temperature difference between the core and the mantle, evaluated at the core-mantle boundary.

The heat flow for all of the models shown in Figure 7 is below the critical value required to sustain thermal convection and thermally driven dynamo action at the present time. Model calculations by Stevenson *et al.* (1983), Schubert and Spohn (1990), and Spohn (1991), using constant mantle viscosity parameterizations, led to much the same conclusion. The models of Breuer and Spohn (2003) predict thermal convection early in Martian history, and are consistent with dynamo action for periods of hundreds of million years, depending on model details such as initial mantle and core temperatures, mantle and core rheology, and the style of heat transfer. These models are consistent with cessation of the dynamo by the time of formation of the Hellas and Isidis basins, providing thermal convection is sufficient to drive the dynamo.

The immobile lid model requires an initial temperature difference between the core and the mantle of a few hundred degrees Kelvin to drive dynamo action, whereas a model with an early era of plate tectonics does not. The stagnant lid model is relatively inefficient at cooling the deep interior of the planet. The necessary temperature difference might arise from superheating the core during core formation. Stevenson (1990) and Nimmo and Stevenson (2000) have argued that this superheating may be difficult to obtain because the iron in the initial iron

silicate mixture might be finely distributed and in thermal equilibrium with the silicates. But Stevenson (2000) has more recently argued for early core superheat to help explain early molten cores.

Convection in the plate tectonics regime brings cold, near surface material to the base of the mantle and cools the core more effectively than stagnant lid convection. As a result, it is more effective in producing core thermal convection and possibly dynamo action. Breuer and Spohn (2003), however, argue that the model with an early plate tectonics episode of mantle convection is difficult to reconcile with the crust formation history of Mars. Geologic evidence (e.g., Frey *et al.*, 2002; Head *et al.*, 2002) suggests that crustal formation and volcanic activity continued well through the Noachian into the Hesperian. Because the early plate tectonics model cools the deep mantle efficiently, it has less potential for widespread volcanic activity after the end of the plate tectonics epoch. The mantle may heat up after cessation of plate tectonics, depending on the heat source inventory and mantle rheology, and may resume volcanic activity. According to Breuer and Spohn (2003), the temperature would peak in the Amazonian, too late to explain the observed crustal formation. Core convection may also be driven by the presence of radiogenic heat sources in the core, as thought possible for the Earth (e.g., Zindler and Hart, 1986; Breuer and Spohn, 1993). Recent studies provide experimental evidence both in support of (Gessmann and Wood, 2002) and contrary to (Chabot and Drake, 1999) this hypothesis.

Chemical convection in the core can drive a dynamo more effectively than thermal convection (e.g., Braginsky, 1964; Stevenson *et al.*, 1983). While the conversion of thermal energy to magnetic field energy is subject to a Carnot efficiency factor, a chemically driven dynamo is not subject to a similar restriction in efficiency. Chemical convection can occur when a solid inner core freezes in a liquid core containing some light, alloying element. Sulfur is usually taken as the most likely candidate because of its cosmochemical abundance and its chemical affinity for iron. If the core has a non-eutectic composition, inner core growth will release buoyant fluid at the surface of the inner core and drive compositional convection even if the core is stably stratified against thermal convection. However, Schubert and Spohn's (1990) thermal evolution models suggest that the present Martian core is likely to be entirely liquid if it contains about 15 weight-% sulfur, as is consistent with the chemistry of SNC meteorites. This would preclude the possibility of compositionally driven convection. A stagnant lid model predicts even higher temperatures in the lower mantle and core and, therefore, strengthens this conclusion.

A present day entirely liquid core also results from the model with an early phase of plate tectonics (Breuer and Spohn, 2003). A stably stratified liquid core at present, but with an early phase of thermal convection and dynamo action, provides a simple explanation for the present absence of a magnetic field at Mars and its early crustal magnetization. However, it is not necessary that the present Martian core be entirely liquid if the compositional dynamo can be otherwise inhibited.

Jault (1996) has suggested that dynamo action may be strongly impeded if an inner solid core grows larger than about 0.35 of the core size.

Evolutionary models both with and without the formation of a solid inner core have been described in recent literature. Formation of an inner core depends on the assumed mantle rheology, liquidus curve (e.g., effect of sulfur on the melting point depression, and how that is calculated), and mode of heat transfer (e.g., plate tectonics or stagnant lid convection). Schubert and Spohn's (1990) model used a relatively stiff rheology (2×10^{21} Pa S at 1600 K) along with Stevenson *et al.*'s (1983) approximation to the liquidus to conclude that a core with 15% sulfur would remain liquid. Longhi *et al.* (1992) used a more sophisticated method due to Williams and Jeanloz (1990) to calculate the liquidus, finding a smaller melting point depression that will favor formation of an inner core. However, the stagnant lid model, with higher temperatures in the mantle and core, results in a liquid core if a similarly stiff rheology is assumed (Breuer and Spohn, 2003). Hauck and Phillips (2002) assumed a relatively weak mantle rheology (10^{19} Pa S at 1600 K) and the Stevenson *et al.* (1983) approximation to the liquidus, finding a molten core at present in their model of Mars evolution. However, had they used the Longhi *et al.* (1992) liquidus, it is likely that a solid inner core would have grown. A present day liquid core also results from models with an early era of plate tectonics, 15% sulfur, a stiff mantle rheology, and the Longhi *et al.* (1992) liquidus (Breuer and Spohn, 2003). It is also possible to have early plate tectonics, form an inner core, and not have a dynamo. In these models the core heats up after the end of the plate tectonics era to a maximum temperature from which it begins to cool. The inner core will keep its radius as long as the core temperature remains below the melting temperature of iron and above the temperature it had at the end of plate tectonics. Inner core growth resumes, along with a chemical dynamo, only when the core temperature falls below its value at the end of the plate tectonics epoch (see also Stevenson, 2001).

Schubert *et al.* (2000) have argued that the remanent magnetization of the crust was acquired much later in Martian history. (See also Stevenson (2001) and Zuber (2001) for a discussion of the timing of the dynamo.) Late magnetization of the crust requires the operation of a strong dynamo after formation of the giant basins, as well as a late addition to the southern highlands crust during the same time. This proposal addresses the observation that not all of the southern highlands crust appears intensely magnetized at this time. Schubert's proposal provides for this by postulating that only the region now characterized by intense magnetization experienced the crustal growth event during the time the dynamo was operative. How this occurred, leaving no visible trace, and why it was confined to specific parts of the southern highlands, remains a mystery.

Schubert's 'late dynamo' proposal allows sufficient time for core solidification to develop as an energy source to power the dynamo. The lack of an operating dynamo today is then attributed to a cessation of inner core growth, e.g., the present core might be either completely frozen or stably stratified and not continuing to

freeze. A recent analysis of MGS radio tracking data yielded an estimate for the tidal Love number k_2 that strongly suggests a fluid or partly fluid core (Yoder *et al.*, 2003) for present day Mars. The Love number is not sensitive enough to the presence and size of a putative inner core, in light of other uncertainties, to distinguish between the two possibilities. The Yoder *et al.* estimate is inconsistent with an earlier analysis (Smith *et al.*, 2001) which found a value of the Love number consistent with a completely solid core. While it is not yet entirely clear, observationally, if all or part of the core remains fluid, the thermodynamic models and arguments described above lead to this expectation. There is also the possibility that the dynamo may not be operative even though the core is freezing and convecting, as suggested by Jault (1996). If sulfur is the light alloying element, then a completely frozen core must be colder than the eutectic temperature of Fe-FeS. The eutectic temperature at Martian core/mantle boundary pressures is between 1400 and 1500 K. This low a temperature is difficult to reconcile with models of the thermal evolution of Mars. It is also difficult to see how the inner core could stop growing as long as the planet cools. If Mars has a partially solidified core at present it must be concluded that solidification of the core is simply not sufficient to sustain dynamo action. Dynamo action is not sufficiently well understood to claim that the presence of an inner solid core requires there to be a dynamo.

Phase transitions in the Martian mantle and their interactions with the mantle flow may provide an alternative explanation for late onset of a purely thermal dynamo that could stop operating similar to the early dynamo discussed above. Spohn *et al.* (1998) have discussed how a putative perovskite layer above the core may affect the thermal history of the core. Such a layer is possible if the Martian core is small and iron-rich so that the pressure in the mantle exceeds the spinel-perovskite transition pressure in the lower mantle (Bertka and Fei; 1997 and Sohl and Spohn; 1997). The perovskite layer could be about 100 to 200 km thick. Since the transition is temperature dependent and has a negative Clapeyron slope it is more likely to occur in early Mars when the mantle temperature was hotter than today. According to 2-D and 3-D convection calculations by Breuer *et al.* (1997), the perovskite layer reduces the heat flow from the core because it forms an additional (convective) layer between the overlying mantle and the core. Therefore, an early perovskite layer would tend to work against an early dynamo. Core superheating during core formation and core heat sources might counter the reduction in core heat flow by such a layer. A perovskite layer could thus be responsible for a late onset of the dynamo, or re-birth of a dynamo, at a later time.

The crystallization ages of the Martian meteorites, except for ALH84001, which is 4.4 billion years old, suggest that they were formed less than about 1 billion years ago. As discussed in Spohn *et al.* (1998), the perovskite layer might thin and eventually disappear as the planet cools. When the perovskite layer becomes so thin that it no longer provides a barrier to the heat flow from the hot core, the layer will become unstable and the core cooling rate will suddenly increase. As a consequence, a thermally driven or chemically driven dynamo could be started or

reactivated. A thermally driven dynamo, as model calculations suggest, could then operate for a few 100 million years before it (again) becomes extinct. A chemically driven dynamo should operate longer, but it would have to cease functioning before the present day.

Models of core evolution are consistent with both an early magnetic field and a late onset magnetic field. These models cannot predict the strength of the magnetic field, but an early dynamo would most likely be driven by relatively inefficient thermal convection while a late onset dynamo would most likely be driven by more efficient chemical compositional convection and latent heat due to inner core freezing. If the core were superheated during its formation, then an early thermally driven dynamo would not require plate tectonics to operate. In this case, a model with a single, immobile plate on top of a convecting mantle can explain early dynamo action, crustal growth, and volcanic activity extending into the Hesperian and beyond, albeit at an ever decreasing rate.

If the magnetization of the crust *postdates* the early Noachian then models with a growing inner core provide an efficient dynamo mechanism but need to explain why and how the dynamo stopped operating. The weak magnetization of the Martian meteorites may suggest a late onset or reactivation of a dynamo that would stop operating before the present. It is also entirely possible that the Martian meteorites were magnetized late in Martian history in the magnetic field of the earlier magnetized crust. More observational data are required to better constrain the history of the magnetic field and the tectonics of Mars.

4. Summary and Conclusions

The discovery of intense crustal magnetization on Mars is one of the most significant surprises of the Mars Global Surveyor era (Stevenson, 2001), one that bodes well for future Mars exploration. Interpretation of the MGS results is still in its infancy, and there is much healthy debate on the interpretation of the observations. As MGS continues to gather data in its mapping orbit, improved global magnetic field maps will become available, and with increasing S/N comes increasing spatial resolution. Some questions may be resolved as the global map comes into better focus, but many will remain, awaiting further observations.

The MGS aerobraking phase offered a tantalizing glimpse of what might be accomplished with a global magnetic field map at low altitude. An orbiter might practically acquire such a map at altitudes of < 150 km, if designed with low drag and/or if fueled to maintain orbit against atmospheric friction. The current MEPAG (Mars Exploration Payload Analysis Group) document identifies such a mission as a next logical step in the exploration of Mars.

The history of Earth Science in the 1960's – and the widespread acceptance of the unifying theory of plate tectonics – was facilitated by the decoding of magnetic records acquired a few km above mid ocean ridges (e.g., Vine and Matthews, 1963).

How exciting it is to imagine what secrets await us at Mars! Access to those secrets will require a magnetic survey with km scale spatial resolution, performed by a low-altitude aerial vehicle or a sufficiently mobile landed vehicle. This too, is a high priority for Mars exploration in the next decade.

Acknowledgements

We thank J. Geiss of the International Space Science Institute in Bern, Switzerland, for hosting the workshop, supported by ISSI, NASA, and the Mars Global Surveyor Project at JPL. We thank our colleagues for helpful discussions, review of the manuscript, and so on. We thank D. Winterhalter of the JPL for organizing the workshop and the workshop proceedings. This research was funded in part by the MGS Project.

References

Acuña, M. H. *et al.*: 1992, 'Mars Observer Magnetic Fields Investigation', *J. Geophys. Res.* **97**, 7799–7814.

Acuña, M. H. *et al.*: 1998, 'Magnetic Field and Plasma Observations at Mars: Initial Results of the Mars Global Surveyor Mission', *Science* **279**, 1676–1680.

Acuña, M. H. *et al.*: 1999, 'Global Distribution of Crustal Magnetism Discovered by the Mars Global Surveyor MAG/ER Experiment', *Science* **284**, 790–793.

Acuña, M. H. *et al.*: 2001, 'The magnetic Field of Mars: Summary of Results from the Aerobraking and Mapping Orbits', *J. Geophys. Res.* **106**, 23403–23417.

Albee, A. L., Palluconi, F. D. and Arvidson, R. E.: 1998, 'Mars Global Surveyor Mission: Overview and Status', *Science* **279**, 1671–1672.

Albee, A. L., Arvidson, R. E., Palluconi, F. D. and Thorpe, T.: 2001, 'Overview of the Mars Global Surveyor Mission', *J. Geophys. Res.* **106**, 23291–23316.

Arkani-Hamed, J.: 2001a, 'A 50-degree Spherical Harmonic Model of the Magnetic Field of Mars', *J. Geophys. Res.* **106**(E10), 23197–23208.

Arkani-Hamed, J.: 2001b, 'Paleomagnetic Pole Positions and Pole Reversals on Mars', *Geophys. Res. Lett.* **28**(17), 3409–3412.

Arkani-Hamed, J.: 2002a, 'An Improved 50-degree Spherical Harmonic Model of the Magnetic Field of Mars Derived from Both High-altitude and Low-altitude Data', *J. Geophys. Res.* **107**(E5).

Arkani-Hamed, J.: 2002b, 'Magnetization of the Mars Crust', *J. Geophys. Res.* **107**(E10).

Bertka, C. M. and Fei, Y.: 1997, 'Mineralogy of the Martian Interior Up to Core-mantle Boundary Pressures', *J. Geophys. Res.* **102**, 5251–5264.

Blakely, R. J.: 1995, *Potential Theory in Gravity and Magnetic Applications*, Cambridge University Press, Cambridge, 437 pp.

Breuer, D. and Spohn, T.: 1993, 'Cooling of the Earth, Urey Ratios, and the Problem of Potassium in the Core', *Geophys. Res. Lett.* **20**, 1655–1658.

Breuer, D., Yuen, D. A. and Spohn, T.: 1997, 'Phase Transitions in the Martian Mantle: Implications for Partially Layered Convection', *Earth Planetary Sci. Lett.* **148**, 457–469.

Breuer, D. and Spohn. T.: 2003, 'Early Plate Tectonics vs. Single Plate Tectonics on Mars: Evidence from Magnetic Field History and Crust Evolution', *J. Geophys. Res.* submitted.

Braginsky, S. I,: 1964, 'Magnetohydrodynamics of the Earth's Core', *Geomag. Aeron.* **4**, 698–712.

Buffett, B. A., Huppert, H. E., Lister, J. R. and Woods, A. W.: 1996, 'On the Thermal Evolution of the Earth's Core', *J. Geophys. Res.* **101**, 7989–8006.

Cain, J. C., Ferguson, B. and Mozzoni, D.: 2002, 'An $n = 90$ Internal Potential Function of the Magnetic Field of the Martian Crustal Magnetic Field', *J. Geophys. Res.* **107**(E10).

Chabot, N. L. and Drake, M. J.: 1999, 'Potassium Solubility in Metal: The Effects of Composition at 15 kbar and 1900 deg C on Partitioning Between Iron Alloys and Silicate Melts', *Earth Planetary Sci. Lett.* **172**, 323–335.

Chen, J. H. and Wasserburg, G. J.: 1986, Formation Ages and Evolution of Shergotty and its Parent Planet from U-Th-Pb Systematics', *Geochim. Cosmochim. Acta* **50**, 955–968.

Christensen, P. R. *et al.*: 2000, 'Detection of Crystalline Hematite Mineralization on Mars by the Thermal Emission Spectrometer: Evidence for Near-surface Water', *J. Geophys. Res.* **105**, 9623–9642.

Cisowski, S. M.: 1986, 'Magnetic Studies on Shergotty and Other SNC Meteorites', *Geochimica and Cosmochimica Acta.* **50**, 1043–1048.

Connerney, J. E. P.: 1993, 'Magnetic Fields of the Outer Planets', *J. Geophys. Res.* **98** (E10), 18,659–18679.

Connerney, J. E. P. *et al.*: 1999, 'Magnetic Lineations in the Ancient Crust of Mars', *Science* **284**, 794–798.

Connerney, J. E. P. *et al.*: 2001, 'The Global Magnetic Field of Mars and Implications for Crustal Evolution', *Geophys. Res. Lett.* **28**, 4015–4018.

Davaille, A. and Jaupart, C.: 1993, 'Transient High-Rayleigh-number Thermal Convection with Large Viscosity Variations', *J. Fluid Mech.* **253**, 141–166.

Dolginov, Sh. Sh. and Zhuzgov, L. N.: 1991, 'The Magnetic Field and Magnetosphere of the Planet Mars', *Planetary Space Sci.* **39**, 1493–1510.

Ernst, R. E., Grosfils, E.B. and Mege, D.: 2001, 'Giant Dike Swarms: Earth, Venus, and Mars', *Ann. Rev. Earth Planetary Sci.* **29**, 489–534.

Fairen, A. G., Ruiz, J. and Anguita, F.: 2002, 'An Origin for the Linear Magnetic Anomalies on Mars Through Accretion of Terranes: Implications for Dynamo Timing', *Icarus* **160**, 220–223.

Frey, H. and Schultz, R. A.: 1988, 'Large Impact Basins and the Mega-impact Origin for the Crustal Dichotomy on Mars', *Geophys. Res. Lett.* **15**, 229–232.

Frey, H. V., Roark, J. H., Shockey, K. M., Frey, E. L. and Sakimoto, S. E. H.: 2002, 'Ancient Lowlands on Mars', *Geophys. Res. Lett.* **29**.

Gessmann, C. K. and Wood, B. J.: 2002, 'Potassium in the Earth's Core?', *Earth Planetary Sci. Lett.* **200**, 63–78.

Glatzmeier, G. A. and Roberts, P. H. 'Simulating the Geodynamo', *Contemp. Phys.* **38**, 269–288.

Goettel, K. A.: 1981, 'Density of the Mantle of Mars', *Geophys. Res. Lett.* **8**, 497–500.

Goldstein, M. L.: 1975, 'Lunar Magnetism', *Nature* **258**, 175.

Grasset, O. and Parmentier, E. M.: 1998, 'Thermal Convection in a Volumetrically Heated, Infinite Prandtl Number Fluid With Strongly Temperature-Dependent Viscosity: Implications for Planetary Thermal Evolution', *J. Geophys. Res.* **103**, 18171–18181.

Gringauz, K. I., Verigin, M., Luhmann, J., Russell, C. T. and Mihalov, J. D.: 1993, 'On the Compressibility of the Magnetic Tails of Mars and Venus', in *Plasma Environments of Non-magnetic Planets*, Pergammon, New York, pp. 265–270.

Hauck, S. A. and Phillips, R. J.: 2002, 'Thermal and Crustal Evolution of Mars', *J. Geophys. Res.* **107**.

Head, J. W., Kreslavsky, M. A. and Pratt, S.: 2002, 'Northern Lowlands of Mars: Evidence for Widespread Volcanic Flooding and Tectonic Deformation in the Hesperian Period', *J. Geophys. Res.* **107**.

Hood, L. L. and Zakharian, A.: 2001, 'Mapping and Modeling of Magnetic Anomalies in the Northern Polar Region of Mars', *J. Geophys. Res.* **106** (E7), 14601–14619.

Jault, D.: 1996, 'Magnetic Field Generation Impeded by Inner Cores of Planets', *Cr. Acad. Sci. II A* **323**, 451–458.

Kellog, O. D.: 1929, *Foundations of Potential Theory*, Frederick Ungar Publishers, New York.

Kleine, T., Münker, C., Metzger and Palme, H.: 2002, 'Rapid Accretion and Core Formation on Asteroids and the Terrestrial Planets from Hf-W Chronometry', *Nature* **418**, 952–955.

Kletetschka, G., Wasilewski, P. J. and Taylor, P. T.: 2000, 'Hematite vs. Magnetite as the Signature for Planetary Magnetic Anomalies?', *Earth Planetary Sci. Lett.* **176**, 469–479.

Langel, R. A.: 1987, in J. A. Jacobs (ed.), 'The Main Field', *Geomagnetism* Academic Press, London, pp. 249–512.

Langel, R. A., Schnetzler, C. C., Phillips, J. D. and Horner, R. J.: 1982, 'Initial Vector Magnetic Anomaly Map from MAGSAT', *Geophys. Res. Lett.* **9**, 273–276.

Langel, R. A. and Estes, H.: 1982, 'A Geomagnetic Field Spectrum', *Geophys. Res. Lett.* **9**, 250–253.

Lee, D. C. and Halliday, A. N.: 1997, 'Core Formation on Mars and Differentiated Asteroids', *Nature* **388**, 854–857.

Leweling, M. and Spohn, T.: 1997, 'Mars: a Magnetic Field Due to Thermoremanence?', *Planetary Space Sci.* **45**, 1389–1400.

Longhi, J., Knittle, E., Holloway, J. R. and Wanke, H.: 1992, in Kieffer, Hugh H., Jakosky, Bruce, M., Snyder, Conway W., Matthews, Mildred S., (Eds), 'The Bulk Composition, Mineralogy, and Internal Structure of Mars', *Mars*, University of Arizona Press, Tucson, AZ, pp. 184–208.

Maus, S., Rother, M., Holme, R., Luhr, H., Olsen, N. and Haak, V.: 2002, 'First Scalar Magnetic Anomaly Map from CHAMP Satellite Data Indicates Weak Lithospheric Field', *Geophys. Res. Lett.* **29** (14).

Maus, S. and Haak, V.: 2002, 'Is the Long Wavelength Crustal Magnetic Field Dominated by Induced or Remanent Magnetization?', *Geophys. Res. Lett.* in press.

Mayhew, M. A. and Galliher, S. C.: 1982, 'An Equivalent Source Magnetization Model for the United States Derived from MAGSAT Data', *Geophys. Res. Lett.* **9**, 311–313.

McSween, H. Y., Jr. *et al.*: 2001, 'Geochemical Evidence Magmatic Water Within Mars from Pyroxenes in the Shergotty Meteorite', *Nature*, **409**, 487–490.

Mitchell, D. L. *et al.*: 2001, 'Probing Mars' Crustal Magnetic Field and Ionosphere with the MGS Electron Reflectometer', *J. Geophys. Res.* **106**(E10), 23419–23427.

Mohlmann, D. *et al.*: 1991, 'The Question of an Internal Martian Magnetic Field', *Planetary Space Sci.* **39**, 83.

Ness, N. F.: 1979, 'The Magnetic Fields of Mercury, Mars and Moon', *Ann. Rev. Earth Planetary Sci.* **7**, 248–288.

Nimmo, F.: 2000, 'Dike Intrusion as a Possible Cause of Linear Martian Magnetic Anomalies', *Geology* **28**, 391–394.

Nimmo, F. and Stevenson, D.: 2000, 'Influence of Early Plate Tectonics on the Thermal Evolution and Magnetic Field of Mars', *J. Geophys. Res.* **105**, 11969–11979.

Ochadlick, A. R., Jr.: 1991, 'Magnetic Exploration of Ocean Crust for Craters of Impact Origin', *Geophysics* **56**(6), 1153–1157.

Olsen, N.: 2002, 'A Model of the Geomagnetic Field and its Secular Variation for Epoch 2000', *Geophys. J. Int.* **149**, 454–462.

Parker, R. L.: 2003, 'Ideal Bodies for Mars Magnetics', *J. Geophys. Res.* **108**(E1).

Purucker, M. *et al.*: 2000, 'An Altitude-normalized Magnetic Map of Mars and Its Interpretation', *Geophys. Res. Lett.* **27**, 2449–2452.

Riedler, W. *et al.*: 1989, 'Magnetic Fields Near Mars: First Results', *Nature* **341**, 604–607.

Roberts, P. H. and Glatzmeier, F. A.: 2000, 'Geodynamo Theory and Ssimulation', *Rev. Modern Physics* **72**, 1081–1123.

Runcorn, S. K.: 1975, 'An Ancient Lunar Magnetic Dipole Field', *Nature* **253**, 701–703.

Runcorn, S. K.: 1975, 'On the Interpretation of Lunar Magnetism', *Phys. Earth planetary Int.* **10**, 327–335.

Russell, C. T.: 1978a, 'The Magnetc Field of Mars: Mars 3 Evidence Re-examined', *Geophys. Res. Lett.* **5**, 81–84.

Russell, C. T.: 1978b, 'The Magnetic Field of Mars: Mars 5 Evidence Re-examined', *Geophys. Res. Lett.* **5**, 85–88.

Russell, C. T.: 1979, in C. F. Kennel (ed.), 'The Interaction of the Solar Wind With Mars, Venus and Mercury', *Solar System Plasma Physics*, North-Holland, Amsterdam, pp. 208–252.

Russell, C. T. *et al.*: 1995, 'A Simple Test of the Induced Nature of the Martian Tail', *Planetary Space Sci.* **43**(7), 875–879.

Schubert, G. and Spohn. T.: 1990, 'Thermal History of Mars and the Sulfur Content of Its Core', *J. Geophys. Res.* **95**, 14095–14104.

Schubert, G, Solomon, S. C., Turcotte, D. L., Drake, M. J. and Sleep,: 1992, in Kieffer, Hugh, H., Jakosky, Bruce M., Snyder, Conway, W., Matthews, Mildred S. (ed.), 'Origin and Thermal Evolution of Mars, *Mars* University of Arizona Press, Tucson, AZ, pp. 147–183.

Schubert, G., Russell, C. T. and Moore, W. B.: 2000, 'Geophysics - Timing of the Martian dynamo', *Nature* **408**, 666–667.

Senshu, H., Kuramoto, K. and Matsui, T.: 2002, 'Thermal Evolution of a Growing Mars', *J. Geophys. Res.* **107**(E12), 5118.

Slavin, J. A., Schwingenschuh, K., Riedler, W. and Yeroshenko, Y.: 1991, 'The Solar Wind Interaction With Mars: Mariner 4, Mars 2, Mars 3, Mars 5, and Phobos 2 Observations of Bow Shock Position and Shape', *J. Geophys. Res.* **96**, 11235–11241.

Slavin, J. A. and Holzer, R. E.: 1994, 'The Solar Wind Interaction With Mars Revisited', *J. Geophys. Res.* **87**, 10285–10296.

Sleep, N. H.: 1994, 'Martian Plate Tectonics', *J. Geophys. Res.* **99**, 5639–5655.

Smith, D. E. *et al.*: 1999, 'The Global Topography of Mars and Implications for Surface Evolution', *Science* **284**, 1495–1503.

Smith, D. E., Zuber, M. T. and Neumann, G. A.: 2001, 'Seasonal Variations of Snow Depth on Mars', *Science* **294**(5549), 2141–2146.

Smith, E. J., Davis, L. Jr., Coleman, P. J. and Jones, D. E.: 1965, 'Magnetic Field Measurements Near Mars', *Science* **149**, 1241–1242.

Sohl, F. and Spohn, T.: 1997, 'The Structure of Mars: Implications from SNC-Meteorites', *J. Geophys. Res.* **102**, 1613–1635.

Solomatov, V. S.: 1995, 'Scaling of Temperature- and Stress-Dependent Viscosity', *Phys. Fluids* **7**, 266–274.

Spohn, T.: 1991, 'Mantle Differentiation and Thermal Evolution of Mars, Mercury, and Venus'. *Icarus* **90**(2), 222–236.

Spohn T., Acuña, M. A., Breuer, D., Golombek, M., Greeley, R., Halliday, A., Hauber, E., Jaumann, R. and Sohl, F.: 2001, 'Geophysical Constraints on the Evolution of Mars', *Space Sci. Rev.* **96**, 231–262.

Spohn, T., Sohl, F. and Breuer, D.: 1998, 'Mars', *Astron. Astrophys. Rev.* **8**, 181–235.

Sprenke, K. F. and Baker, L. L.: 2000, 'Magnetization, Paleomagnetic Poles, and Polar Wander on Mars', *Icarus* **147**, 26–34.

Stevenson, D. J., Spohn, T. and Schubert, G.: 1983, 'Magnetism and Thermal Evolution of the Terrestrial Planets', *Icarus* **54**, 466–489.

Stevenson, D. J.: 1990, in Newsom, H. E., Jones, J. H. (eds), 'Fluid dynamics of core formation. *Origin of the Earth* Oxford University Press, New York, pp. 231–249.

Stevenson, D. J.: 2001, 'Mars Core and Magnetism', *Nature* **412**, 214–219.

Stevenson, D. J.: 2000, 'Core Superheat', *EOS Trans. AGU* **81** (48).

Telford, W. M., Geldart, L. P., Sheriff, R. E. and Keys, D. A.: 1976, *Applied Geophysics*, Cambridge University Press, Cambridge.

Verigin, M. I. *et al.*: 1991, 'Ions of Planetary Origin in Martian Magnetosphere', *Planetary Space Sci.* **39** (1–2), 131–137.

Voorhies, C. V., Sabaka, T. J. and Purucker, M.: 2002, 'On Magnetic Spectra of Earth and Mars', *J. Geophys. Res.* **107** (E6).

Wadhwa, M.: 2000, 'Redox State of Mars' Upper Mantle and Crust From Eu Anomalies in Shergottite Pyroxenes', *Science* **291**, 1527–1530.

Wihelms, D. E. and Squyres, S. W.: 1984, 'The Martian Hemispheric Dichotomy May be Due to a Giant Impact', *Nature* **309**, 138–140.

Williams, Q. and Jeanloz, R.: 1990, 'Melting Relations in the Iron Sulfur System at Ultra-high Pressures: Implications For the Thermal State of the Earth', *J. Geophys. Res.* **95**, 19299–19310.

Wise, D. U., Golombeck, M. P. and McGill, G. E.: 1979, 'Tectonic Evolution on Mars', *J. Geophys. Res.* **84**, 7934–7939.

Zindler, A. and Hart, S.: 1986, 'Chemical Geodynamics', *Ann. Rev. Earth Planetary Sci.* **14**, 493–571.

Yoder, C. F., Konopliv, A. S., Yuan, D. N., Standish, E. M. and Folkner, W. M.: 2003, 'Fluid Core Size of Mars from Detection of the Fluid Tide', *Science*.

Zuber, M. T.: 2001, 'The Crust and Mantle of Mars', *Nature* **412**, 220–227.

Zuber, M. T., Solomon, S. C., Phillips, R. J., Smith, D. E., Tyler, G. L., Aharonson, O., Balmino, G., Banerdt, W. B., Head, J. W., Lemoine, F. G., McGovern, P. J., Neumann, G. A., Rowlands, D. D. and Zhong, S.: 2000, 'Internal Structure and Early Thermal Evolution of Mars from Mars Global Surveyor Topography and Gravity', *Science* **287**, 1788–1793.